

Figure S1. Gating strategies and examples of CD3⁺ T cells, CD19⁺ B cells, CD14⁺ monocytes and CD56⁺CD3⁻ NK cells. FS, forward scatter; NK, natural killer; SS, side scatter.

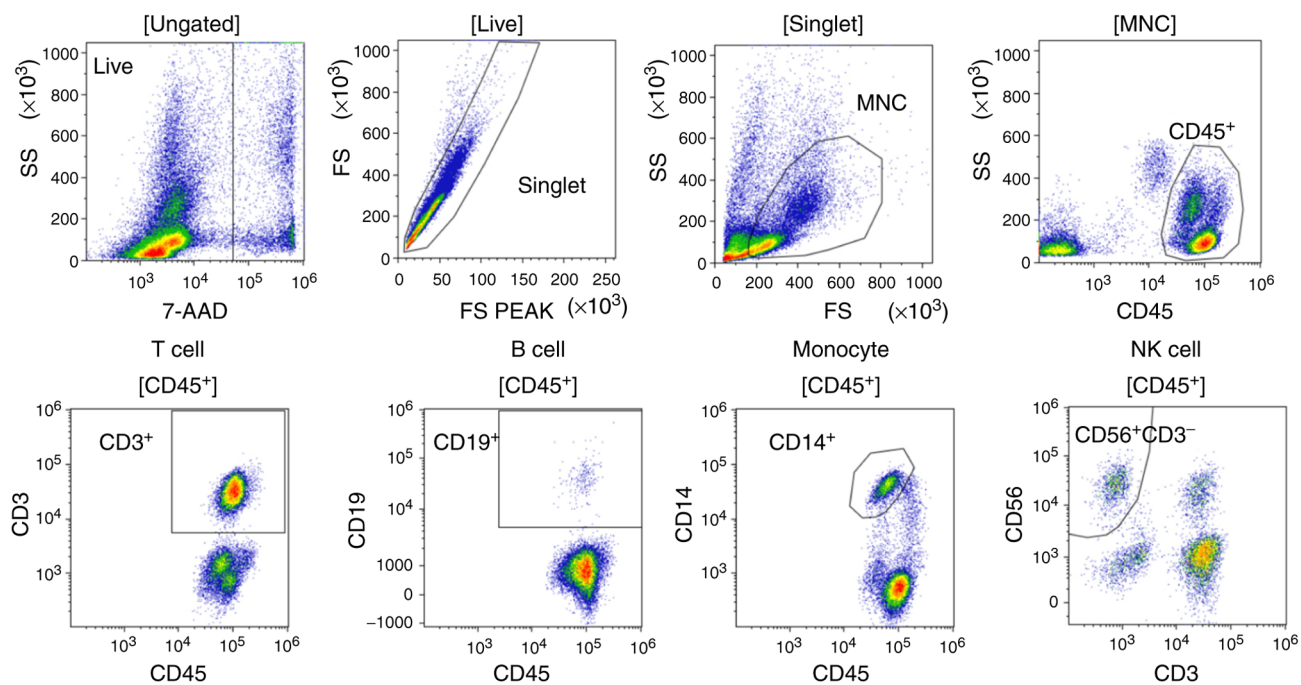


Figure S2. Examples of CD56⁺CD3⁻ NK cells. Pre-treatment and post-treatment peripheral blood mononuclear cells were compared. NK, natural killer.

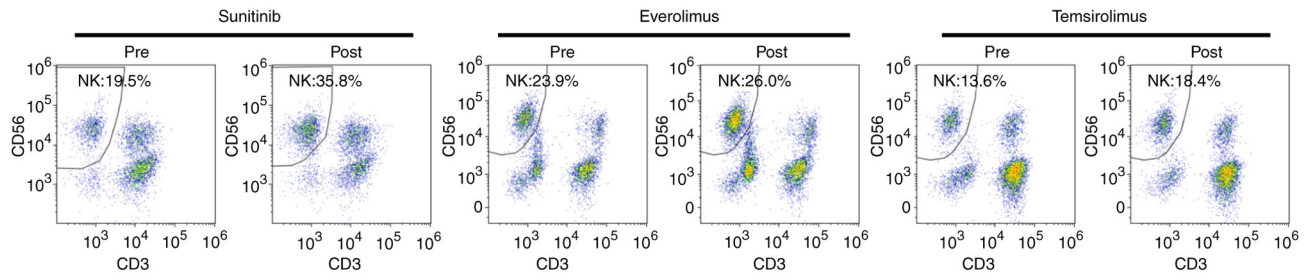


Figure S3. Gating strategies and examples of CD45RA and CCR7 expression on CD8⁺ and CD4⁺ T cells. CCR7, C-C chemokine receptor type 7; FS, forward scatter; SS, side scatter.

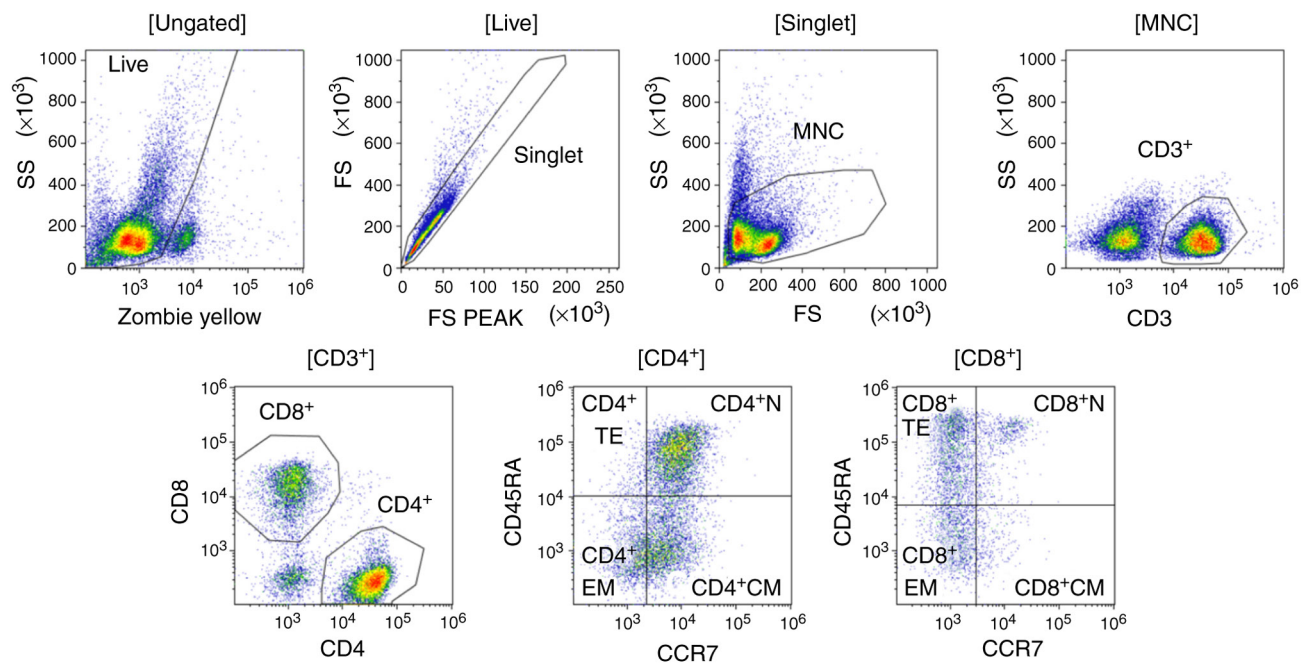


Figure S4. Examples of PD-1, TIM-3 and LAG-3 expression on (A) CD4⁺ and (B) CD8⁺ T cells.

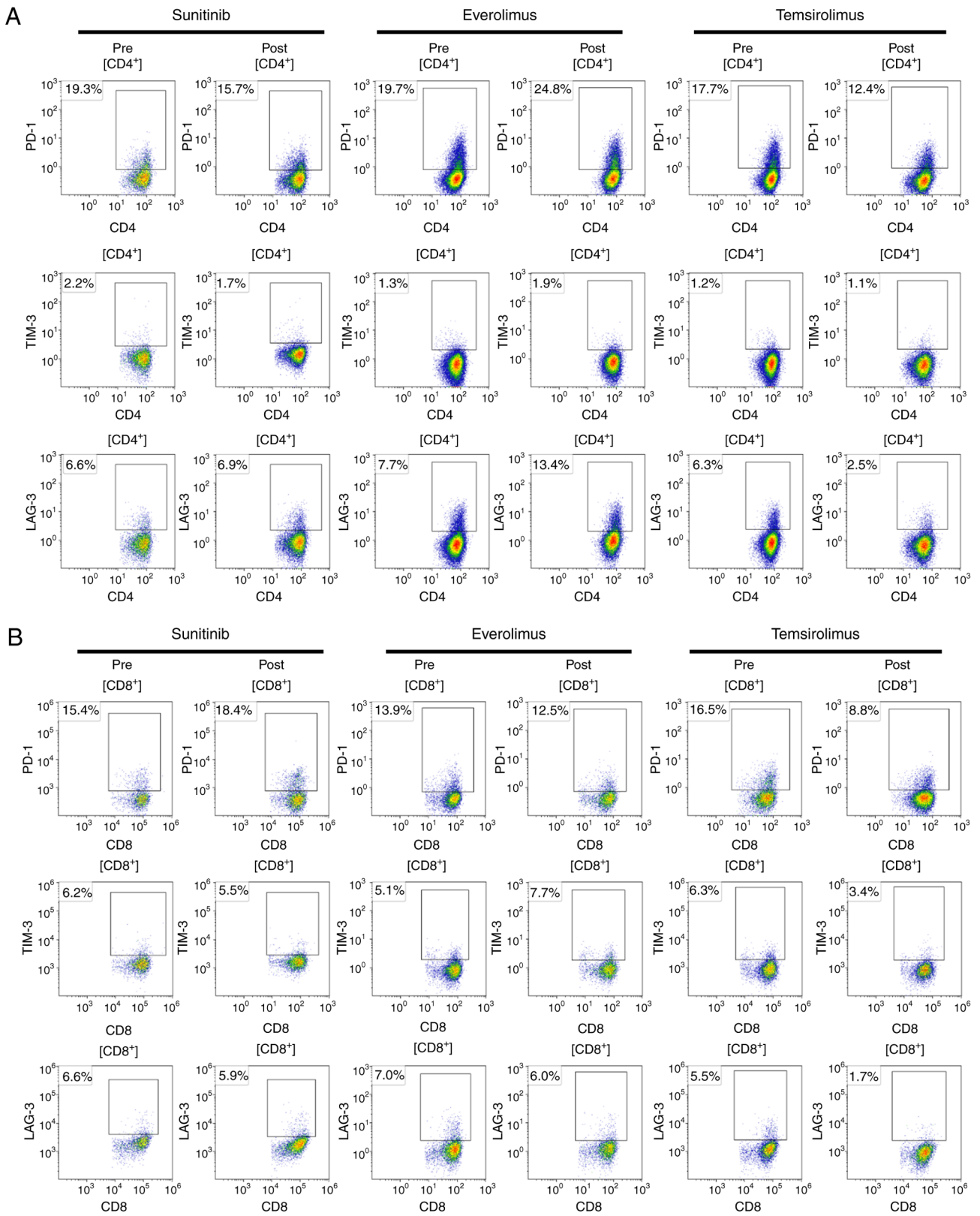


Figure S4. Continued. Pre-treatment and post-treatment peripheral blood mononuclear cells were compared. Examples of NKG2D, DNAM1, and CD95 expression on (C) CD4⁺ and (D) CD8⁺ T cells. Pre-treatment and post-treatment PBMCs were compared. DNAM1, DNAX accessory molecule 1; LAG-3, lymphocyte activation gene 3 protein; PD-1, programmed cell death protein 1; TIM-3, T cell immunoglobulin and mucin protein 3.

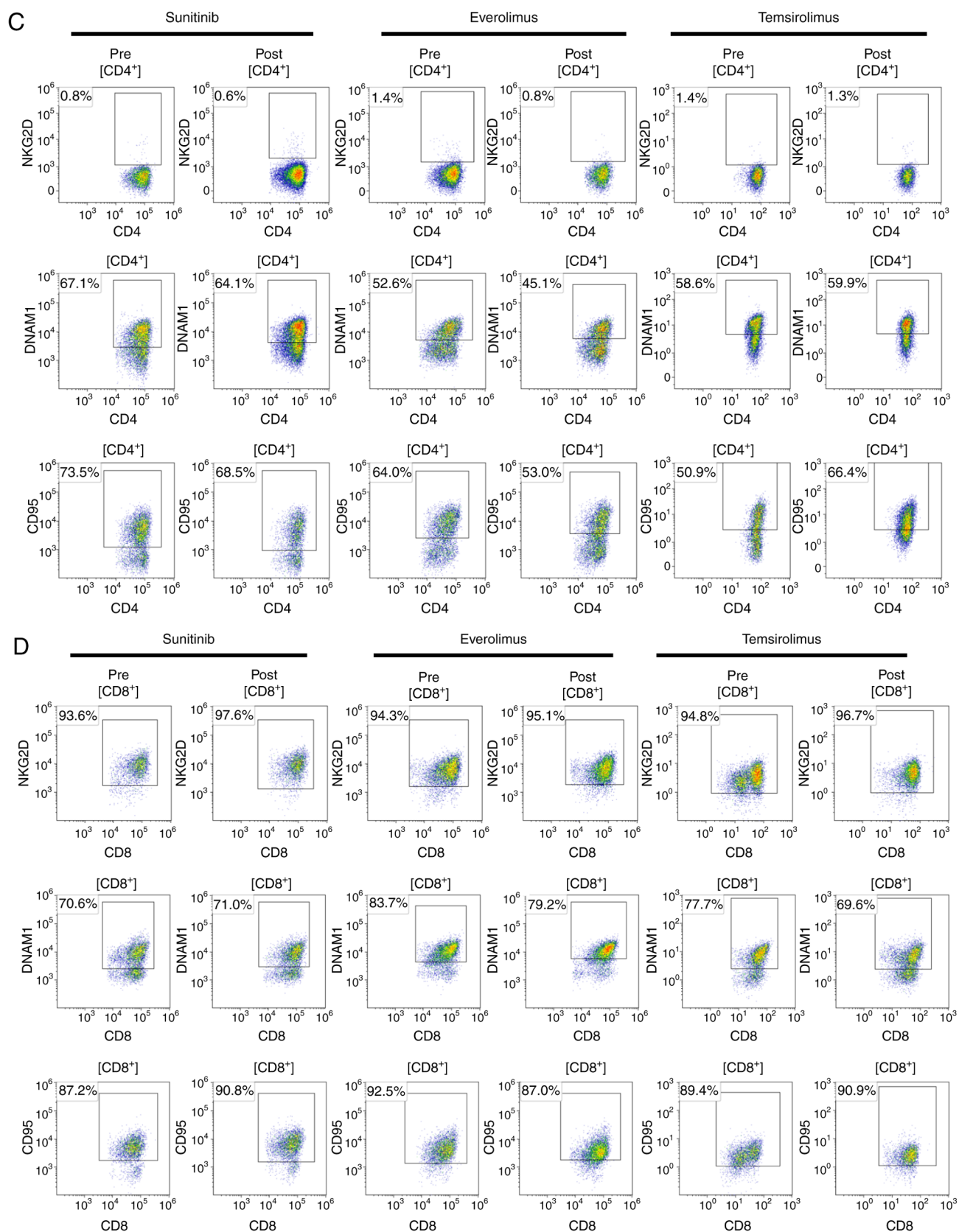


Figure S5. Gating strategies and examples of CD45RA-FOXP3^{high} effector regulatory T cells. FOXP3, forkhead box P3; FS, forward scatter; MNC, mononuclear cell; SS, side scatter.

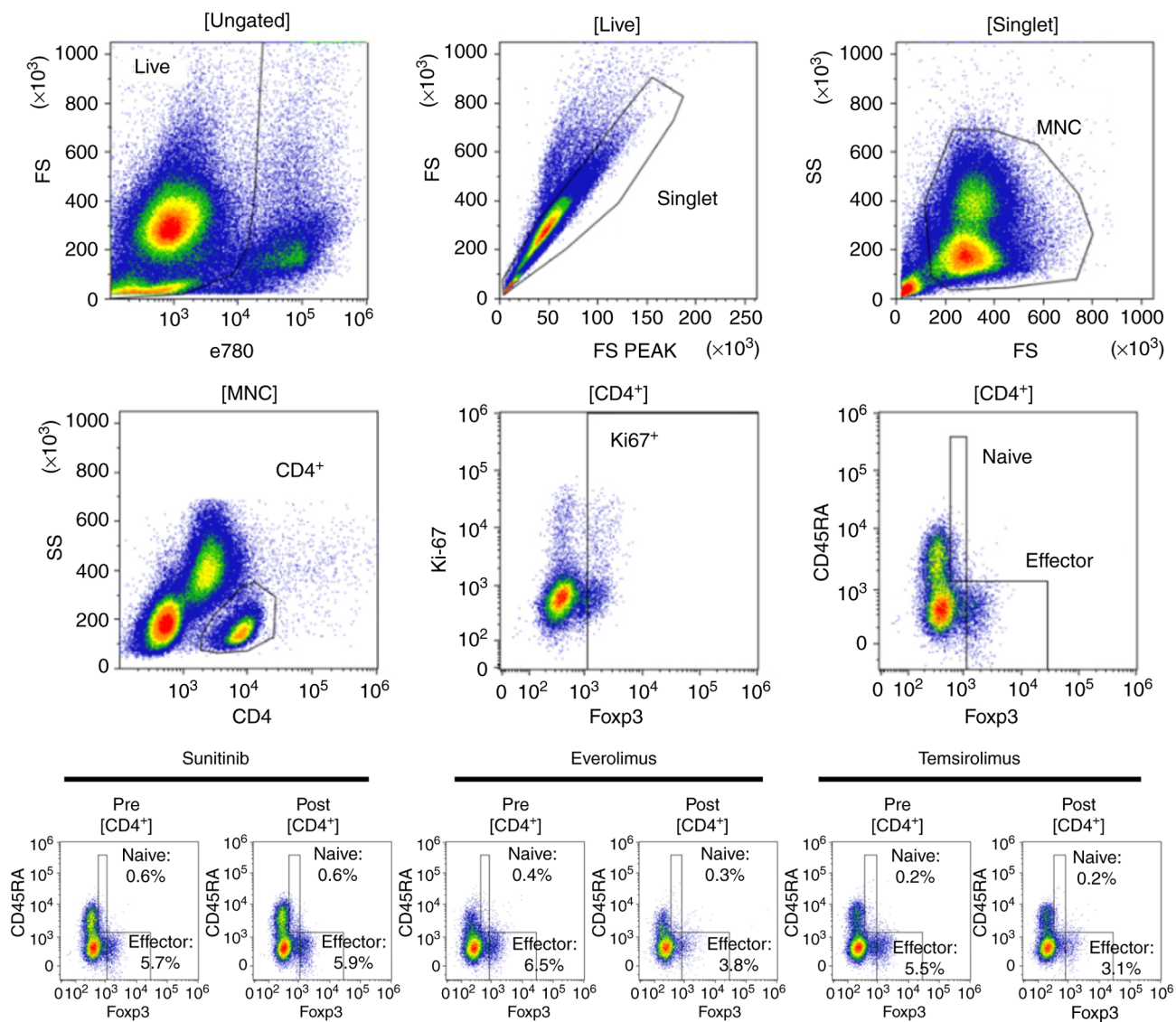


Figure S6. Gating strategies for Lin(CD3CD19CD20CD56)CD11b⁺CD14⁺CD15⁻HLA-DR⁻CD33⁺ monocytic MDSCs and Lin⁻CD14⁻CD15⁻HLA-DR⁻CD33⁺ early-stage MDSCs. FS, forward scatter; HLA-DR, human leukocyte antigen-DR; MDSCs, myeloid-derived suppressor cells; SS, side scatter.

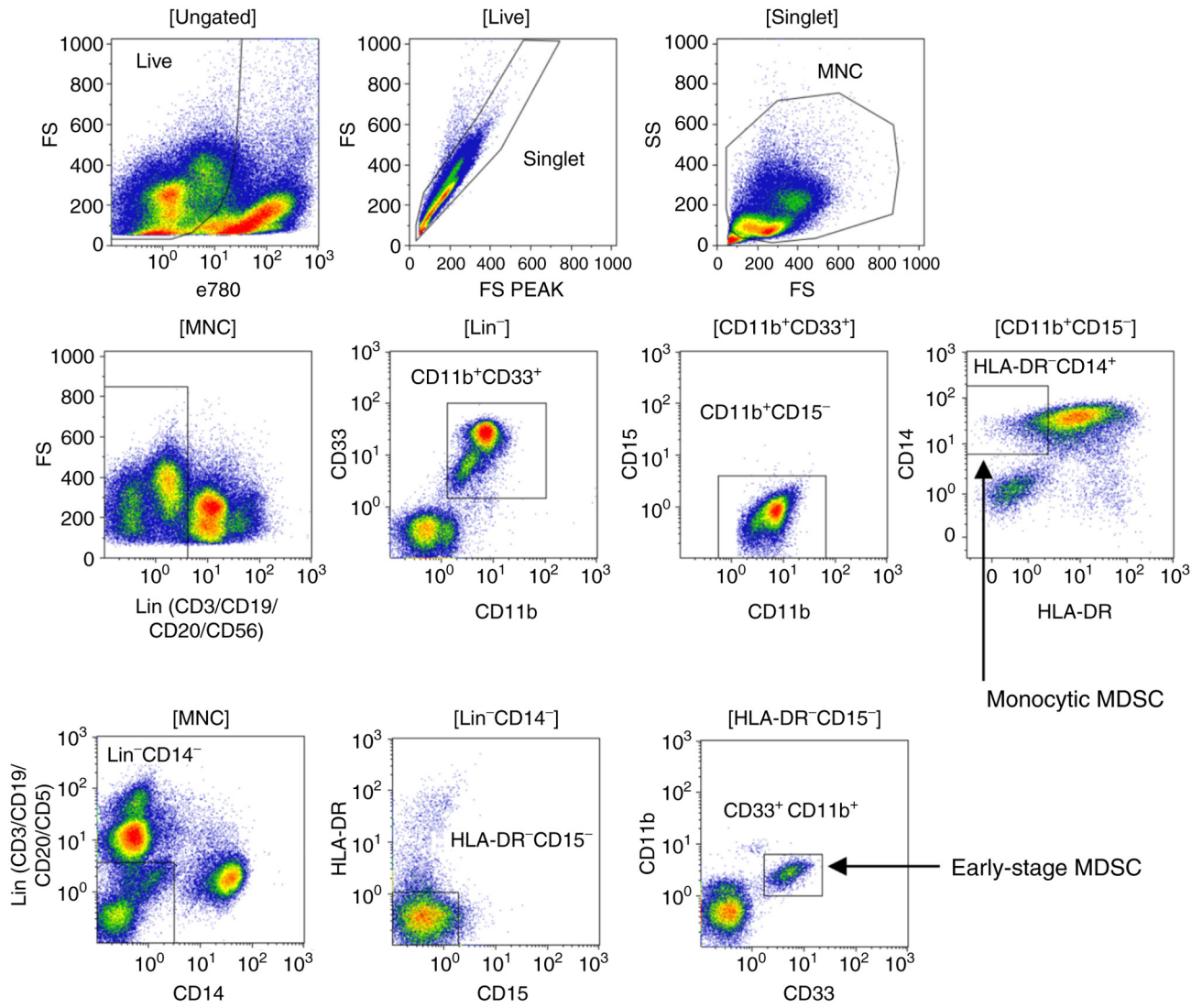


Figure S7. Examples of (A) M-MDSCs and (B) eMDSCs. Pre-treatment and post-treatment peripheral blood mononuclear cells were compared. eMDSCs, early-stage MDSCs; HLA-DR, human leukocyte antigen-DR; M-MDSCs, monocytic MDSCs; MDSCs, myeloid-derived suppressor cells.

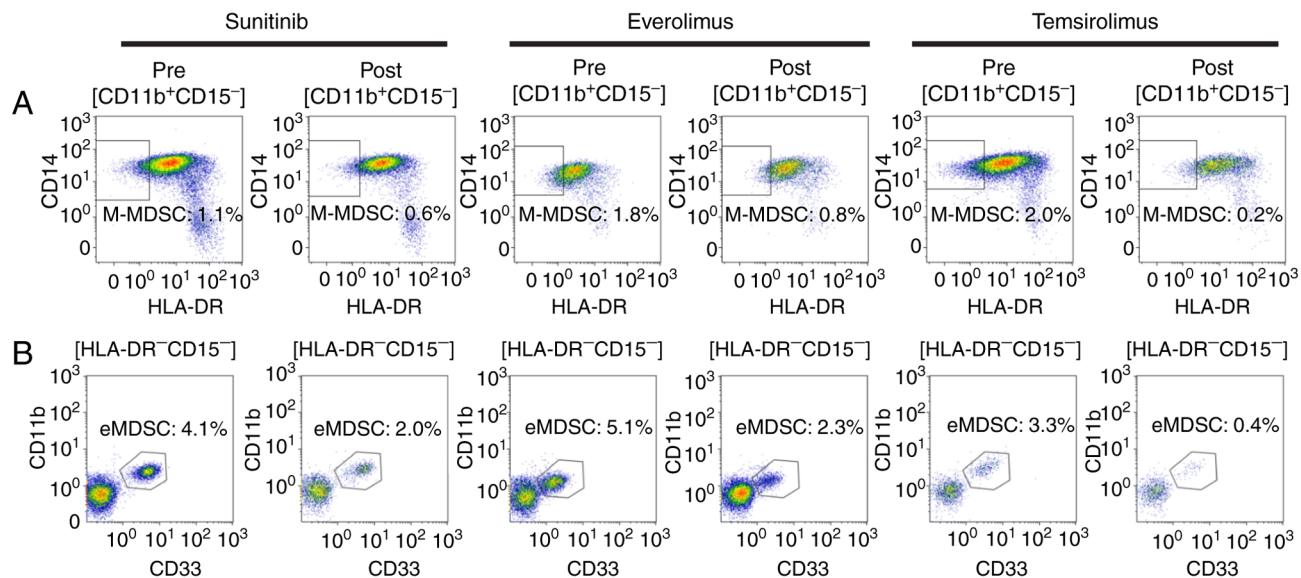


Figure S8. Gating strategies and examples of CD28⁺CD57⁺KLRG1⁺CD3⁺ immunosenescent T cells. Pre-treatment and post-treatment peripheral blood mononuclear cells were compared. FS, forward scatter; SS, side scatter.

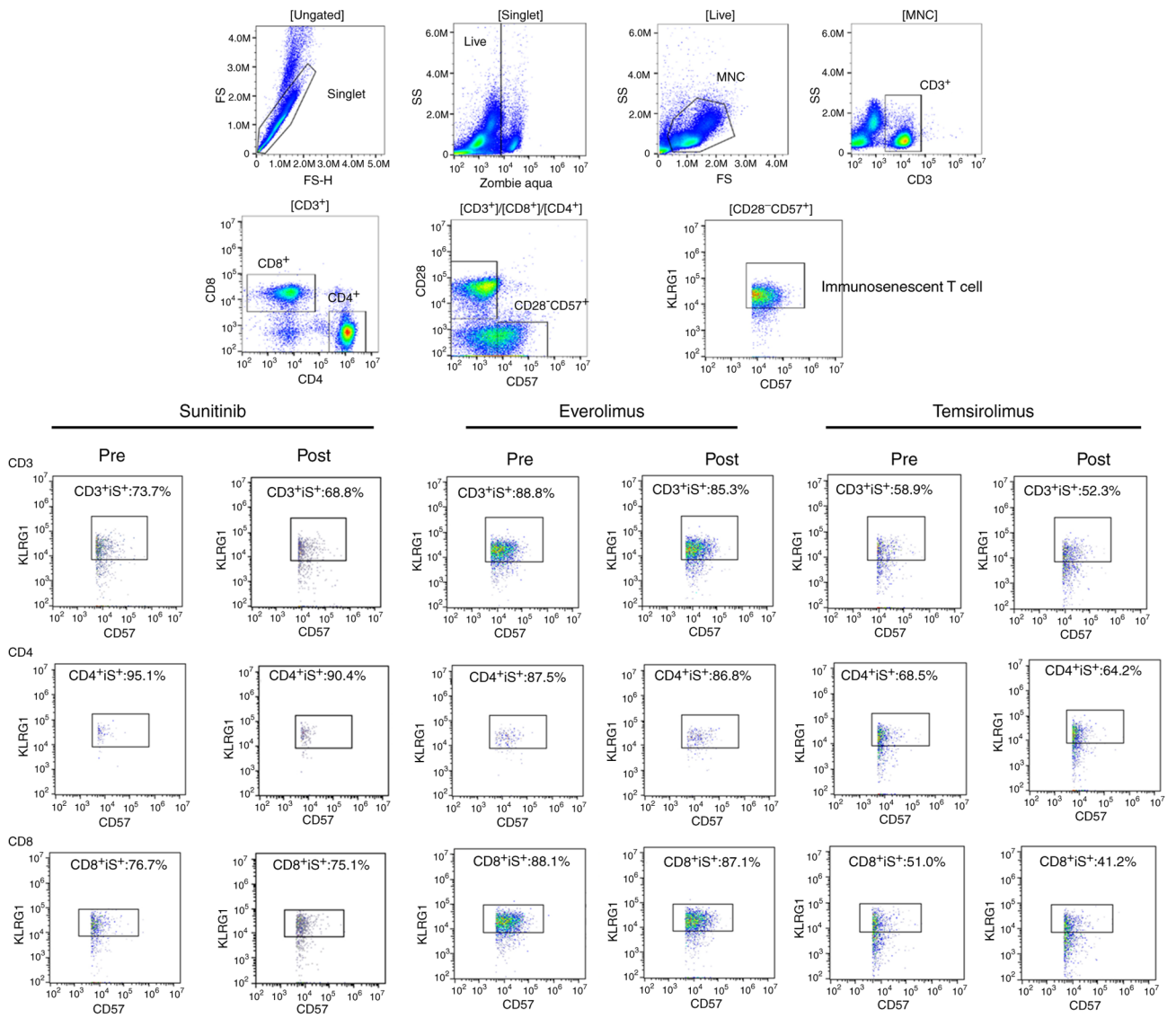


Figure S9. Glucose uptake and mitochondrial staining. (A) CD4⁺ and CD8⁺ T cells were gated as indicated. Histograms for (B) 2-NBDG, (C) MTG and (D) TMRE staining were shown. 2-NBDG, 2-deoxy-2-[(7-nitro-2,1,3-benzoxadiazol-4-yl) amino]-D-glucose; FS, forward scatter; MTG, MitoTracker Green; SS, side scatter; TMRE, tetramethylrhodamine, ethyl ester.

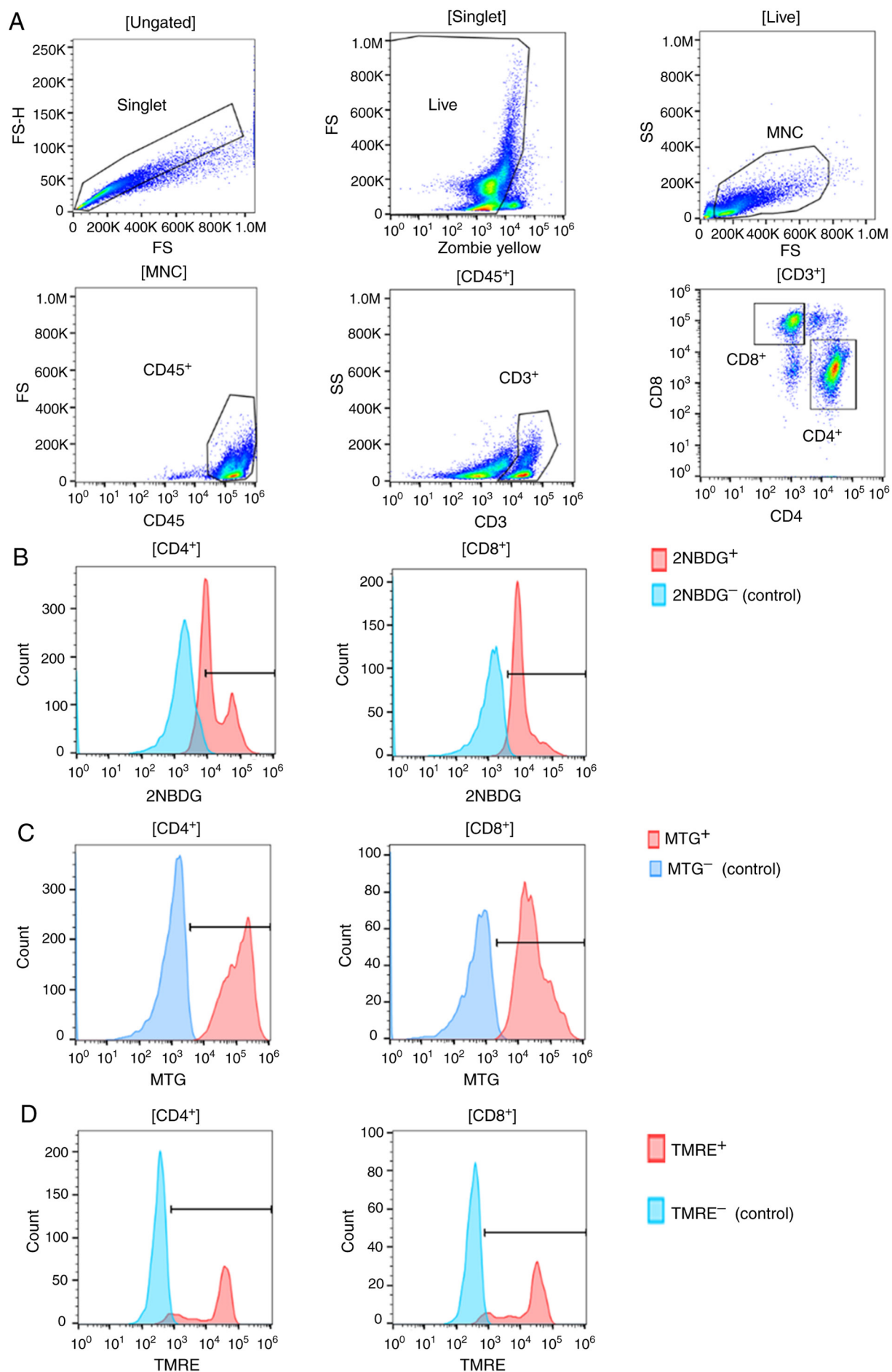


Figure S10. Examples of 2-NBDG, MTG and TMRE staining before treatment in red and after treatment in blue. 2-NBDG, 2-deoxy-2-[(7-nitro-2,1,3-benzoxadiazol-4-yl) amino]-D-glucose; MTG, MitoTracker Green; SS, side scatter; TMRE, tetramethylrhodamine, ethyl ester.

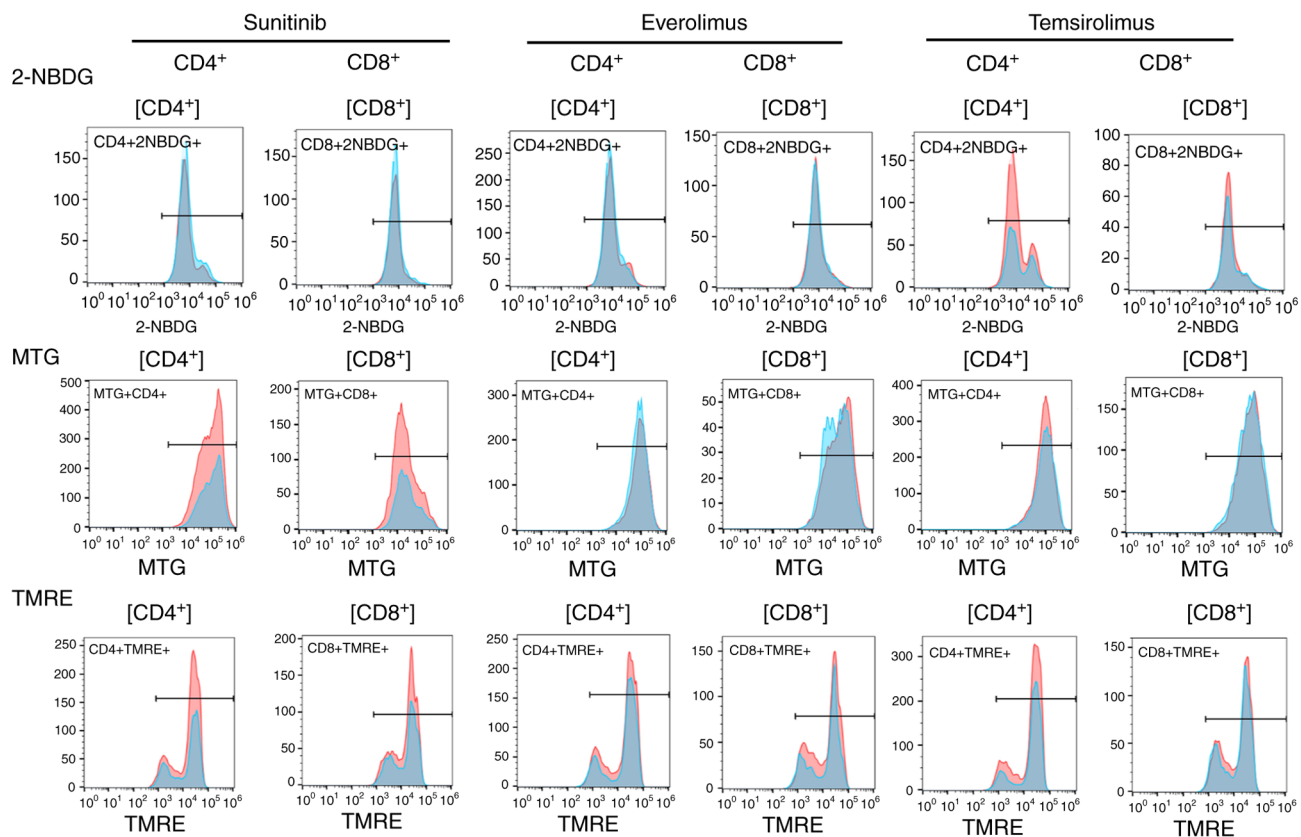


Figure S11. Gating strategy for cytokine-producing T cells by intracellular cytokine staining. FS, forward scatter; IFN- γ , interferon- γ ; MNC, mononuclear cell; SS, side scatter; TNF- α , tumor necrosis factor- α .

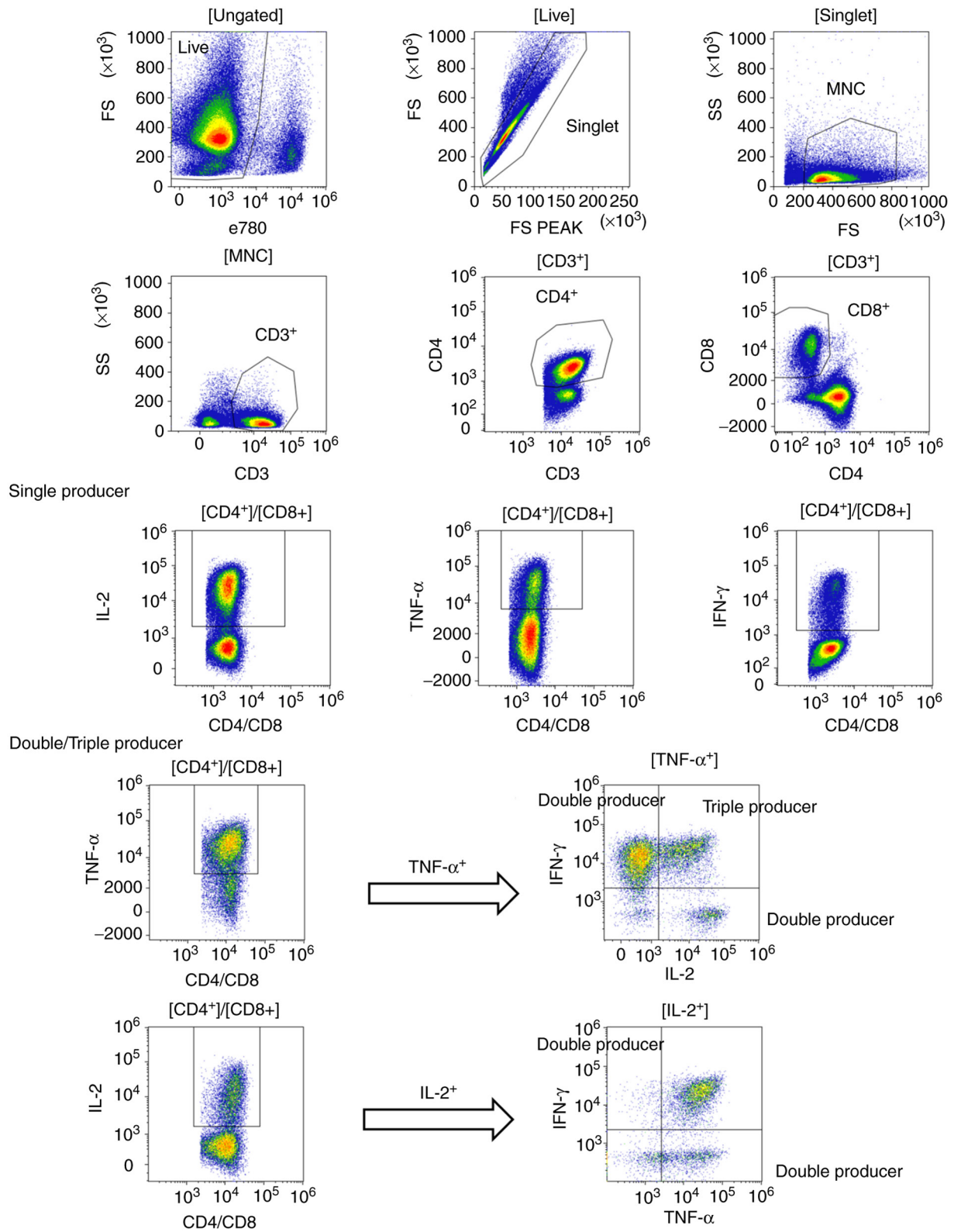


Figure S12. Examples of cytokine-producing (A) CD4⁺ and (B) CD8⁺ T cells. Pre-treatment and post-treatment peripheral blood mononuclear cells were compared. IFN- γ , interferon- γ ; TNF- α , tumor necrosis factor- α .

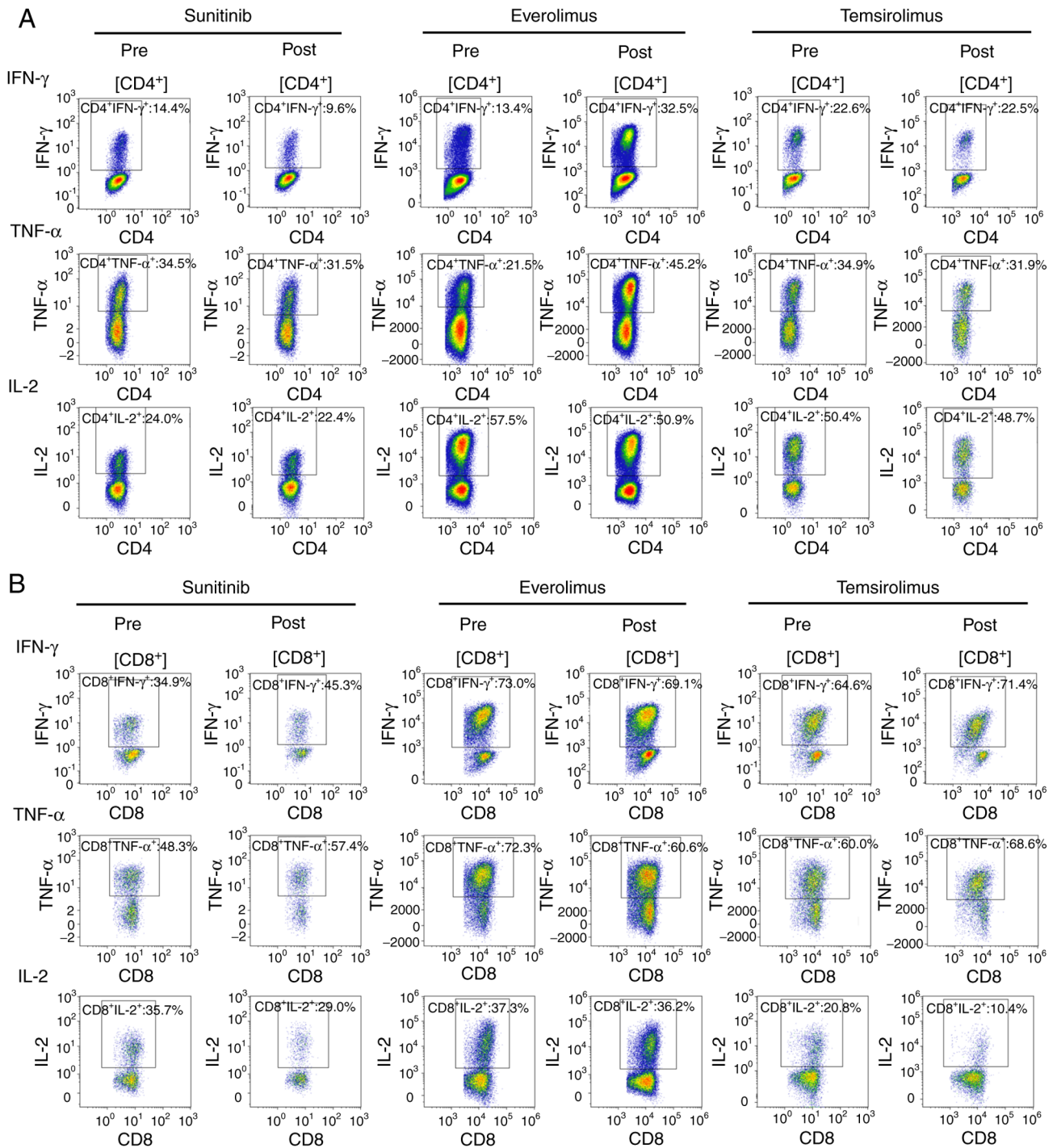


Figure S13. Examples of polyfunctional or dysfunctional (A-C) CD4⁺ and (D-F) CD8⁺ T cells. (A and D) IL-2-IFN- γ ⁺TNF- α ⁺ double producer and (B and E) dysfunctional T cells. (C and F) The number of cytokine-producing cells was shown in pie charts. Pre-treatment and post-treatment peripheral blood mononuclear cells were compared. IFN- γ , interferon- γ ; TNF- α , tumor necrosis factor- α .

